

## Accepted Manuscript

Title: Minimum centroid neighborhood for minimum zone sphericity

Author: Andrea Rossi Stefano Chiodi Michele Lanzetta

PII: S0141-6359(13)00181-5  
DOI: <http://dx.doi.org/doi:10.1016/j.precisioneng.2013.11.004>  
Reference: PRE 6059

To appear in: *Precision Engineering*

Received date: 11-7-2013  
Revised date: 7-11-2013  
Accepted date: 17-11-2013



Please cite this article as: Rossi A, Chiodi S, Lanzetta M, Minimum centroid neighborhood for minimum zone sphericity, *Precision Engineering* (2013), <http://dx.doi.org/10.1016/j.precisioneng.2013.11.004>

This is a PDF file of an unedited manuscript that has been accepted for publication. As a service to our customers we are providing this early version of the manuscript. The manuscript will undergo copyediting, typesetting, and review of the resulting proof before it is published in its final form. Please note that during the production process errors may be discovered which could affect the content, and all legal disclaimers that apply to the journal pertain.

# Minimum centroid neighborhood for minimum zone sphericity

*Andrea Rossi, Stefano Chiodi and Michele Lanzetta*

Department of Civil and Industrial Engineering

University of Pisa, Largo Lazzarino, 56122 Pisa, Italy

Email: lanzetta@unipi.it tel.: +39 050 2218122 fax: +39 050 2218065

## Abstract

The minimum zone sphericity tolerance is derived from the ANSI and ISO standards for roundness and has extensive applications in the tribology of ball bearings, hip joints and other lubricated pairs. The worst-case proposed in this paper provides theoretical evidence that the minimum zone center of the two (circumscribed and inscribed reference) spheres with minimum radial separation containing the sampled spherical surface is included in a spherical neighborhood centered in the centroid of radius  $2\pi^{-2}E_C$ , where  $E_C$  is the sphericity error related to the centroid, which can be determined in closed form.

Such linear estimating (about 20% of  $E_C$  from the centroid, i.e. about one order of magnitude lower than the sphericity tolerance to be assessed) can be used to locate the sphere center with a given tolerance and as a search neighborhood for minimum zone center-based algorithms, such as metaheuristics (genetic algorithms, particle swarm optimization etc.). The proposed upper bound has been experimentally assessed, using a genetic algorithm (GA) with parameters previously optimized for roundness and extended to three dimensions, which has overcome most of all available datasets from the literature that have been tested with center-based minimum zone algorithms by different authors. The optimum dataset size on artificially generated datasets is also discussed and it is speculated to allow the extension of the proposed upper bound to partial (or incomplete) spherical features.

**Keywords:** form error, minimum zone sphericity (MZS), Chebyshev criterion, search neighborhood, upper bound, least squares method, metaheuristics, genetic algorithm (GA), CMM

## 1. Introduction

Sphericity affects the functional properties, e.g. tribology and lubrication, of various mechanical devices, such as ball bearings, hip joints and other spherical couplings and lubricated pairs.

According to ANSI [1], sphericity shares the same definition with circularity for form error evaluation from ISO [2]. The sphericity evaluation involves the determination of two concentric spheres, the circumscribed and inscribed (reference) spheres to the sampled points dataset (substitute feature), such that the radial separation between these two spheres is minimum (Figure 1): minimum zone sphericity (MZS).

The evaluation of sphericity based on the minimum zone criterion is a non-linear and non-convex problem.

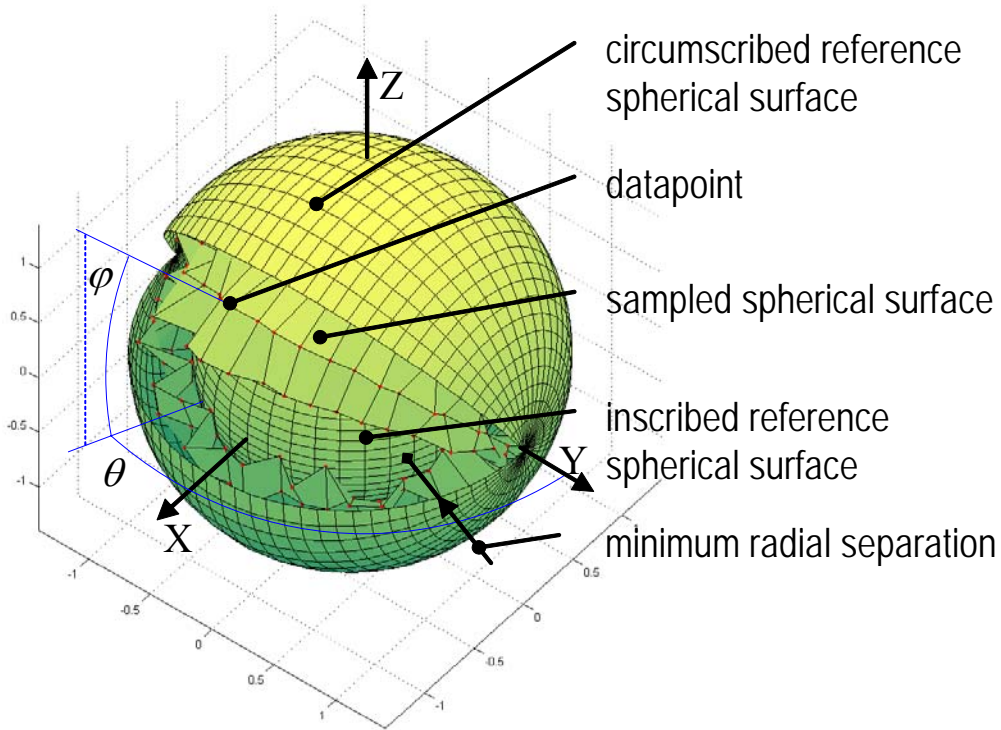


Figure 1: The reference system and feature. The minimum zone sphericity error  $E_{MZ}$  is the minimum radial separation between the two concentric spherical surfaces respectively circumscribed and inscribed to the sampled dataset, centered in the (unknown) minimum zone center  $C_{MZ}$ .

About here

Some approaches to the MZS problem are based on the minimization of the minimum zone error  $E_{MZ}$  as a function of the minimum zone center  $C_{MZ}$ . The inconvenience is that this function has several local minima; consequently, the exploration is computationally intensive. The main purpose of current work is the definition and reduction of a search area for the  $C_{MZ}$ .

Some examples of center-based approaches are the simplex search / linear approximation [3] [4] and metaheuristics like the particle swarm optimization (PSO) [5] [6], ant systems [7], evolutionary [8] and genetic algorithms (GAs) [9] [10] [11] [12].

Sphericity can be evaluated by roundness (or circularity) in different equatorial sections of the sphere surface.

Exact methods were proposed to evaluate sphericity based on the minimum zone criterion, such as [13], which is based on Voronoi tessellation, however this method is computationally intensive and it is not applicable to partial (or incomplete) spherical surfaces.

Fan and Lee [14] proposed an approach with minimum potential energy analogy to the minimum zone solution of spherical form error. The problem of finding the minimum zone sphericity error is transformed into that of finding the minimum elastic potential energy of the corresponding mechanical system. Chen [15] constructed three mathematical models to evaluate the minimum circumscribed sphere, the maximum inscribed sphere and the minimum zone sphere by directly resolving the simultaneous linear algebraic equations first. Then, the minimum zone solutions can be obtained using only five datapoints, which verify the 4-1, the 1-4, the 3-2 or the 2-3 condition.

Samuel and Shunmugam [16] established a minimum zone limaçon based on computational geometry to evaluate roundness error; with geometric methods, global optima are found by exhaustively checking every local minimum candidate.

Most of these methods process data point-by-point in the parameter space and move between datapoints by using some transition rules following the given nonlinear constraints one at a time. The point-to-point search method is sometime dangerous, because it is very possible to allocate false peaks in the multimodal search space for nonlinear optimization problems [17].

The main purpose of this work is to provide in closed form the minimum neighborhood of the centroid  $C$  that includes the minimum zone center  $C_{MZ}$  (Figure 2). The definition of a restricted spherical volume centered in the centroid of the sampled sphere, which certainly includes the minimum zone center, has several applications: it can be used (i) *tout court* as a conservative first estimation of the minimum zone center position and of the minimum zone error; (ii) it may define a search neighborhood for a local search, e.g. by metaheuristics, such as genetic algorithms, particle swarm optimization etc. By reducing the search area, the algorithm complexity and the computation time can be reduced [18]. Apart from [18], which uses a qualitatively adaptable search space size, in the literature only the following are available: [19] uses a fixed 1 mm search space size with a GA; [8] uses a fixed 2 mm search space size with an immune evolutionary algorithm; and later reduces the search space size to 0.1 mm with PSO [20]. All use the least squares center as the search space center. Fixed search space size poses, on one hand, the risk that the minimum zone center may not be included, particularly with partial features or non-uniformly distributed sampled points; on the other hand, too large search spaces increase the complexity and processing time.

## 2. Problem formulation

The MZT is the solution of the following optimization problem [11]:

$$\min \left[ \max_{\theta_i = i \frac{2\pi}{n}, i=1, \dots, n, \varphi_j = j \frac{2\pi}{n}, j=1, \dots, \frac{n}{2}} s(x, y, z, \theta_i, \varphi_j) - \min_{\theta_i = i \frac{2\pi}{n}, i=1, \dots, n, \varphi_j = j \frac{2\pi}{n}, j=1, \dots, \frac{n}{2}} s(x, y, z, \theta_i, \varphi_j) \right] \quad (1)$$

subject to  $(x, y, z) \in S$

where  $S$  is the search-space,  $\theta_i = i \frac{2\pi}{n}$ ,  $\varphi_j = j \frac{2\pi}{n} - \frac{\pi}{2}$ ,  $i=0, \dots, n$ ,  $j=1, \dots, \frac{n}{2}$  are the angular locations of *equiangular* data of the sphericity surface  $s(x, y, z, \theta_i, \varphi_j)$  of the sphere of center  $(x, y, z)$ .

The solution of problem (1) is the minimum zone error  $E_{MZ}$  defined as:

$$\begin{aligned} E_{MZ} &= R_{\max}(C_{MZ}) - R_{\min}(C_{MZ}) = \\ &= \max_{\theta_i = i \frac{2\pi}{n}, i=1, \dots, n, \varphi_j = j \frac{2\pi}{n}, j=1, \dots, \frac{n}{2}} s(C_{MZ}, \theta_i, \varphi_j) - \min_{\theta_i = i \frac{2\pi}{n}, i=1, \dots, n, \varphi_j = j \frac{2\pi}{n}, j=1, \dots, \frac{n}{2}} s(C_{MZ}, \theta_i, \varphi_j) \end{aligned} \quad (2)$$

where  $C_{MZ} = (x_{MZ}, y_{MZ}, z_{MZ})$  is the unknown minimum zone center.

## 3. An upper bound for the centroid to minimum zone center distance

In this section, we will provide the minimum distance between the minimum zone center  $C_{MZ}$  defined above and the centroid  $C$ .

For this estimation, a worst-case inspired from [21] is proposed, which explores additional properties that can be extended to current problem. The worst-case is based on the geometrical feature  $F(\alpha)$  formed by two concentric-opposite spherical sectors shown in Figure 2 and described by:

$$F(\alpha) = \left\{ \begin{array}{l}
(r \cdot \cos\varphi \cdot \cos\theta, r \cdot \cos\varphi \cdot \sin\theta, r \cdot \sin\varphi) \equiv (r, 0, 0), \quad \theta=0, \varphi=0 \\
(R \cdot \cos\varphi \cdot \cos\theta, R \cdot \cos\varphi \cdot \sin\theta, R \cdot \sin\varphi), \quad \left( \alpha \in \left[ 0, \frac{\pi}{2} \right], \theta \in \left[ -\frac{\pi}{2} - \alpha, \frac{\pi}{2} + \alpha \right], \forall \varphi \right) \vee \\
\quad \left( \alpha \in \left[ 0, \frac{\pi}{2} \right], \theta \in \left[ \frac{\pi}{2} + \alpha, \frac{3\pi}{2} - \alpha \right], \varphi \in \left[ \frac{\pi}{2} - \alpha - |\pi - \theta|, \frac{\pi}{2} \right] \vee \varphi \in \left[ -\frac{\pi}{2}, -\frac{\pi}{2} + \alpha + |\pi - \theta| \right] \right) \vee \\
\quad \left( \alpha \in \left[ -\frac{\pi}{2}, 0 \right], \theta \in \left[ -\frac{\pi}{2} - \alpha, \frac{\pi}{2} + \alpha \right], \varphi \in \left[ -\frac{\pi}{2} - \alpha + |\theta|, \frac{\pi}{2} + \alpha - |\theta| \right] \right) \\
(r \cdot \cos\varphi \cdot \cos\theta, r \cdot \cos\varphi \cdot \sin\theta, r \cdot \sin\varphi), \quad \left( \alpha \in \left[ 0, \frac{\pi}{2} \right], \theta \in \left( \frac{\pi}{2} + \alpha, \frac{3\pi}{2} - \alpha \right), \varphi \in \left( -\frac{\pi}{2} + \alpha + |\pi - \theta|, \frac{\pi}{2} - \alpha - |\pi - \theta| \right) \right) \vee \\
\quad \left( \alpha \in \left[ -\frac{\pi}{2}, 0 \right], \theta \in \left( -\frac{\pi}{2} - \alpha, \frac{\pi}{2} + \alpha \right), \varphi \in \left( \frac{\pi}{2} + \alpha - |\theta|, \frac{\pi}{2} \right) \vee \varphi \in \left( -\frac{\pi}{2}, -\frac{\pi}{2} - \alpha + |\theta| \right) \right) \vee \\
\quad \left( \alpha \in \left[ -\frac{\pi}{2}, 0 \right], \theta \in \left( \frac{\pi}{2} + \alpha, \frac{3\pi}{2} - \alpha \right), \forall \varphi \right)
\end{array} \right.$$

(3)

where  $r_{\min} < r < R$ ,  $-\frac{\pi}{2} \leq \alpha < \frac{\pi}{2}$ ,  $r_{\min}$  is defined by (19) below and  $(r, 0, 0)$  is a *control point*,

which makes the feature open in  $\theta = \varphi = 0$ .

It will be proven that, by construction, the control point generally forces the minimum zone center  $C_{MZ}$  in the origin  $(0, 0, 0)$  (if the conditions of *Lemma 3* below are satisfied).

As for  $\alpha$ , it results that  $F(\alpha=0)$  is formed by *two concentric-opposite half spherical surfaces*;

$F\left(\frac{\pi}{2}\right)$  is a spherical surface of radius  $R$ ; and,  $F\left(-\frac{\pi}{2}\right)$  is a spherical surface of radius  $r$ .

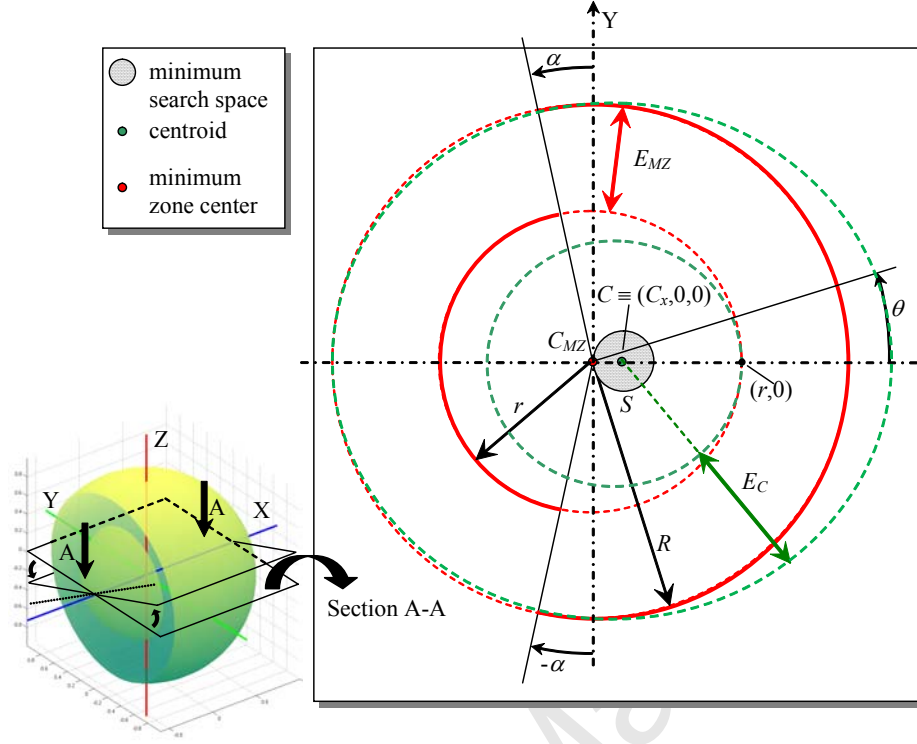


Figure 2: Worst-case for the maximum distance (enhanced for clarity) between centroid  $C$  and minimum zone center  $C_{MZ}$ .

About here

The considered feature is axial symmetrical with respect to the X-axis (inset of Figure 2).

A number of properties of  $F(\alpha)$  is given. They can be applied for each feature defined by expression

(3) and rotated by  $\frac{k}{2\pi}$ ,  $0 \leq k < 2\pi$ .

The worst-case for the centroid to minimum zone center distance is obtained when the asymmetry of the feature  $F(\alpha)$  in Figure 2 is maximized. Let  $F_r(\alpha)$  and  $F_R(\alpha)$  be the component features of radii  $r$  and  $R$ , respectively, at the left and at the right side of  $F(\alpha)$ . For  $\alpha > 0$  ( $\alpha < 0$ ),  $F(\alpha)$  is obtained by  $F(0)$  removing (adding) an axially symmetric feature on the  $X^-$ -axis ( $X^+$ -axis). The maximum asymmetry of  $F(\alpha)$  about the Y-axis is achieved by setting  $\alpha = 0$ . As it will be proven in the

following *Lemma 1*, if  $\alpha > 0$ ,  $F_r(\alpha)$  evaluated for  $\frac{\pi}{2} \leq \theta \leq \frac{\pi}{2} + \alpha$  is mirrored with respect to the YZ-

plane to  $F_R(\alpha)$  evaluated for  $\frac{\pi}{2} - \alpha \leq \theta \leq \frac{\pi}{2}$ . Analogously if  $\alpha < 0$ ,  $F_R(\alpha)$  evaluated for  $\alpha \leq \theta \leq \frac{\pi}{2}$

is mirrored to  $F_r(\alpha)$  evaluated for  $\frac{\pi}{2} + \alpha \leq \theta \leq \pi$ .

Increasing the asymmetry of  $F(\alpha)$  about the YZ-plane, the centroid  $C$  moves away from the minimum zone center  $C_{MZ}$ .

*Lemma 1.* The two concentric-opposite half spherical surfaces of  $F(0)$  maximize the distance  $C_x$  (on the X-axis) between the centroid  $C \equiv (C_x, 0, 0)$  and the origin  $(0, 0, 0) \equiv C_{MZ}$ .  $\square$

*Proof.* Without loss of generality for the feature symmetry about the X-axis for all sections of  $F(\alpha)$  parallel to the XY-plane, at the Z coordinate  $R \sin \varphi$ , the centroid abscissa is

$$C_x = \frac{\int_{\frac{\pi}{2}-\alpha}^{\frac{\pi}{2}+\alpha} R \cdot \cos \varphi \cdot \cos \theta \cdot d\theta + \int_{\frac{\pi}{2}+\alpha}^{\frac{3\pi}{2}-\alpha} r \cdot \cos \varphi \cdot \cos \theta \cdot d\theta}{\int_0^{2\pi} d\theta} = \frac{R \cdot \cos \varphi \cdot \sin \theta \Big|_{\frac{\pi}{2}-\alpha}^{\frac{\pi}{2}+\alpha} + r \cdot \cos \varphi \cdot \sin \theta \Big|_{\frac{\pi}{2}+\alpha}^{\frac{3\pi}{2}-\alpha}}{2\pi} =$$

$$= \frac{2R \cdot \cos \varphi \cdot \cos \alpha - 2r \cdot \cos \varphi \cdot \cos \alpha}{2\pi} = \frac{(R-r) \cos \varphi \cos \alpha}{\pi}$$

(4)

which is maximized for  $\alpha = 0 \mid \forall \varphi$ .

This conclusion, valid for all the two-dimensional sections of the considered feature  $F(0)$  parallel to section A-A in Figure 2, is also valid for the whole three-dimensional feature  $F(0)$  obtained by the integration of all the considered sections.  $\blacksquare$

Since  $C_x$  for  $\alpha=0$  is the upper bound for the centroid to minimum zone center distance, in the remainder only  $F(0)$  is considered, although most of the following geometric assumptions are valid for  $F(\alpha)$ .

*Corollary 1.* The highest distance between the centroid  $C$  and the origin  $(0, 0, 0) \equiv C_{MZ}$  is achieved when  $r$  is low ( $r_{\min}$ ) with respect to  $R$ .

*Lemma 2.* The centroid of  $F(0)$  is

$$C = \left( 2 \frac{R-r}{\pi^2}, 0, 0 \right) \quad (5)$$

$\square$



*Proof.*  $F(0)$  is formed by two half spherical surfaces of radii  $R$  and  $r$  and the centroids of these half

spherical surfaces are located on the X-axis respectively at  $C_R = \frac{\int_{-\pi/2}^{\pi/2} \int_{-\pi/2}^{\pi/2} R \cdot \cos\varphi \cdot \cos\theta \cdot d\varphi d\theta}{\int_{-\pi/2}^{\pi/2} \int_{-\pi/2}^{\pi/2} d\varphi d\theta} = \frac{4R}{\pi^2}$  and

$$C_r = \frac{\int_{\pi/2}^{3\pi/2} \int_{-\pi/2}^{\pi/2} r \cdot \cos\varphi \cdot \cos\theta \cdot d\varphi d\theta}{\int_{\pi/2}^{3\pi/2} \int_{-\pi/2}^{\pi/2} d\varphi d\theta} = -\frac{4r}{\pi^2}.$$

Obviously, the control point  $(r,0,0)$  has a negligible weight in the evaluation of  $C$ .

$$C_x = \frac{C_R + C_r}{2} = 2 \frac{R-r}{\pi^2} \quad (6)$$

■

After discussing the position of the centroid  $C$  with respect to the origin for the proposed worst-case feature  $F(0)$ , the conditions to force the position of the minimum zone center  $C_{MZ}$  in the origin are represented in Figure 3 and discussed below.

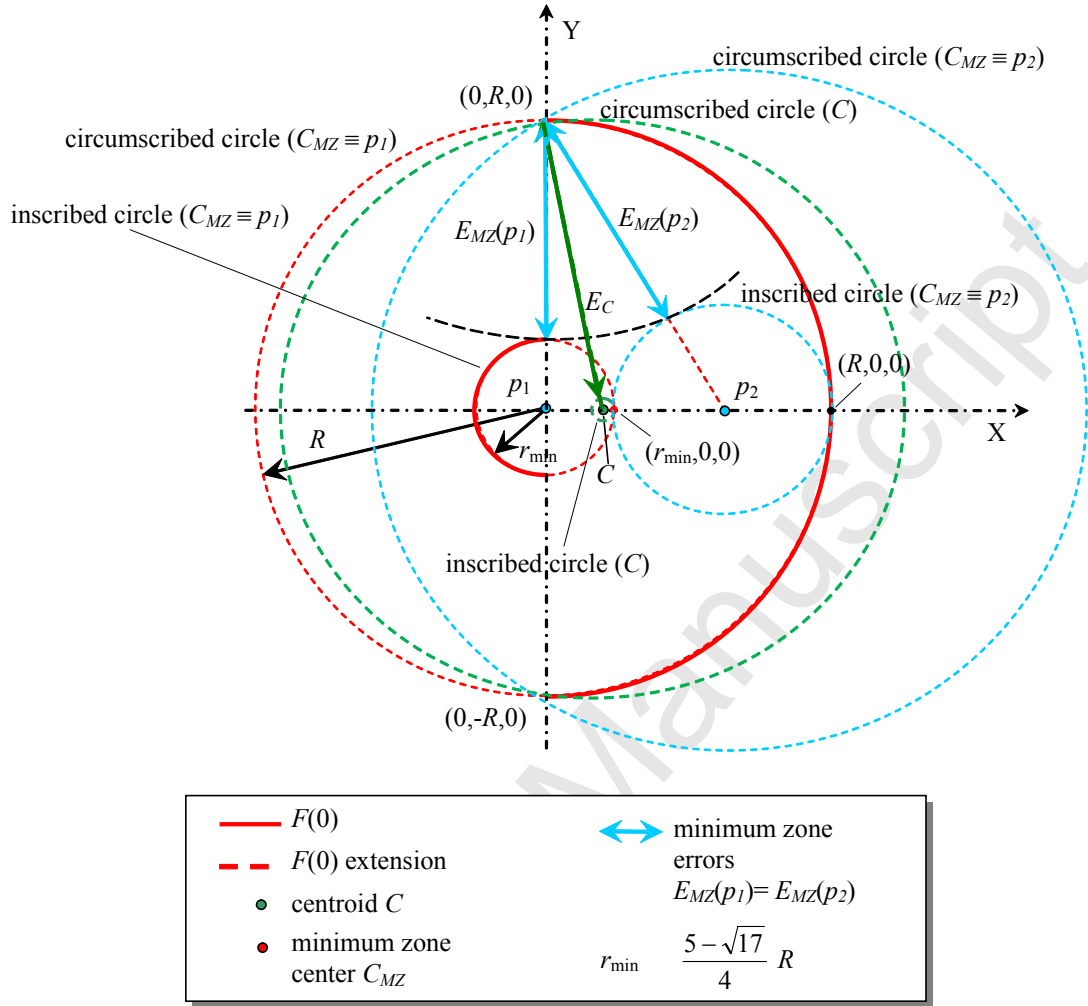


Figure 3: Condition on the minimum  $r$  ( $r_{\min}$  of the worst-case feature  $F(0)$ ) to keep the minimum zone center  $C_{MZ}$  in position  $p_1$ , the origin of axes, before jumping in position  $p_2$ .

About here

It can be noticed that for  $r$  high enough with respect to  $R$ :

- $C_{MZ}$  is located in  $p_1=(0,0,0)$  because the geometry of  $F(0)$  is made up of the circumscribed reference spherical surface (of radius  $R$ ) and of the inscribed reference spherical surface (of radius  $r$ ).

As for the minimum zone error of the feature  $F(0)$ , according to (2)

$$E_{MZ} = R - r \quad (7)$$

Vice versa, for lower  $r$  with respect to  $R$  (also for  $r \rightarrow 0$ ):

- $C_{MZ}$  is located in  $p_2 = (\frac{R+r}{2}, 0, 0)$ , because the circumscribed reference spherical surface crosses the Y-axis at  $(0, R, 0)$ ,  $(0, -R, 0)$  and  $(0, 0, R)$  and the inscribed reference spherical surface crosses the X-axis at points  $(r, 0, 0)$  and  $(R, 0, 0)$  (according to the 3-2 model [15]); and

$$E_{MZ} = \sqrt{\left(\frac{R+r}{2}\right)^2 + R^2} - \left(\frac{R-r}{2}\right) \quad (8)$$

The following lemma defines the conditions on the  $\frac{r}{R}$  ratio influencing the  $C_{MZ}$  in position  $p_1$  (or  $p_2$ ).

*Lemma 3.* The minimum zone center  $C_{MZ}$  of the feature  $F(0)$  is in the  $p_1 = (0, 0, 0)$ , if and only if  $C_{MZ} \equiv p_1 = (0, 0, 0) \Leftrightarrow E_{MZ} = R - r$  (9)

where the ratio  $\frac{r}{R}$  is a solution of the equation

$$2\left(\frac{r}{R}\right)^2 - 5\frac{r}{R} + 1 \leq 0 \quad (10)$$

otherwise, if

$$2\left(\frac{r}{R}\right)^2 - 5\frac{r}{R} + 1 > 0 \quad (11)$$

$$C_{MZ} \equiv p_2 = \left(\frac{R+r}{2}, 0, 0\right) \quad (12)$$

□

*Proof.* By the definition of minimum zone center  $E_{MZ}$  in (2),  $C_{MZ} \equiv p_1$  if and only if the following condition is verified:

$$R_{\max}(p_1) - R_{\min}(p_1) \leq R_{\max}(p_2) - R_{\min}(p_2) \quad (13)$$

From expressions (7) and (8), the left and right terms become

$$R-r \leq \sqrt{\left(\frac{R+r}{2}\right)^2 + R^2} - \left(\frac{R-r}{2}\right) \quad (14)$$

finally

$$3\left(1 - \frac{r}{R}\right) \leq \sqrt{5 + 2\frac{r}{R} + \left(\frac{r}{R}\right)^2} \quad (15)$$

$$2\left(\frac{r}{R}\right)^2 - 5\frac{r}{R} + 1 \leq 0$$

■

*Corollary 2.* As  $\frac{r}{R} < 1$  by construction, the interval of feasible solutions of expression (15) is

$$\frac{5 - \sqrt{17}}{4} \leq \frac{r}{R} < 1 \quad (16)$$

because the contiguous interval

$$1 \leq \frac{r}{R} \leq \frac{5 + \sqrt{17}}{4} \quad (17)$$

includes unfeasible solutions for  $F(0)$ .

The boundary condition on  $\frac{r}{R}$  for  $C_{MZ}$  to move from  $p_1$  to  $p_2$  is given by

$$\frac{r}{R} = \frac{5 - \sqrt{17}}{4} \quad (18)$$

It seems that a spherical feature with  $\frac{r}{R}$  as low as about 0.2 provided by (16) and (18) yielding a

larger search space has no practical interest for the assessment of the sphericity tolerance.

Consequently, for the sake of straightforwardness of presentation, the case of  $C_{MZ} = p_2$  is not discussed, and in (3) for  $F(\alpha)$

$$r_{\min} = \frac{5 - \sqrt{17}}{4} R \quad (19)$$

The boundary condition in (18) and (19) for  $\frac{r}{R}$  is valid for both 2D (roundness) [21] and 3D (sphericity) features because the  $C_{MZ}$  position only depends on the ratio between the two radiuses. The closed form upper bound of the distance  $C_x$  between the centroid  $C$  and the minimum zone center  $C_{MZ}$  can be formulated as a function of the roundness error  $E_C$  related to the centroid  $C$  given by the following *Theorem*.

*Theorem*

$$\max C_x = \max_{F(0)} |C - C_{MZ}| \leq 2\pi^{-2} E_C \quad (20)$$

□

From *Corollary 1* the centroid to minimum zone center distance  $C_x$  is maximized when  $r$  is minimized. From *Lemma 3* and *Corollary 2* this occurs when  $r_{\min} = \frac{5 - \sqrt{17}}{4} R$ :

$$\max C_x = \max_{F(0)} |C - C_{MZ}| = \max_{r \geq \left(\frac{5 - \sqrt{17}}{4}\right)R} 2 \frac{R - r}{\pi^2} = 2 \frac{R - r_{\min}}{\pi^2} = \frac{\sqrt{17} - 1}{2\pi^2} R \cong 0.15822 R \quad (21)$$

However, equation (8) can be used to evaluate a lower bound of  $E_C$ . In fact, for *Lemma 3* and *Corollary 2*,  $p_2$  is a minimum zone center about the just after the border  $r_{\min} = \frac{5 - \sqrt{17}}{4} R$  and for definition of minimum zone error  $E_{MZ}$  every other error is higher; particularly the one with respect to the centroid. It results:

$$\begin{aligned}
E_C &\geq R_{\max}(p_2) - R_{\min}(p_2) = \\
&= \sqrt{\left(\frac{R+r}{2}\right)^2 + R^2} - \left(\frac{R-r}{2}\right) = \\
&= R \left( \sqrt{\left(\frac{1+\frac{r}{R}}{2}\right)^2 + 1} - \left(\frac{1-\frac{r}{R}}{2}\right) \right) = \\
&= \frac{R}{2} \left( \sqrt{5 + 2\frac{r}{R} + \left(\frac{r}{R}\right)^2} - 1 + \frac{r}{R} \right) \geq \\
&\geq \frac{R}{2} \left( \sqrt{5 + \frac{5-\sqrt{17}}{2} + \left(\frac{5-\sqrt{17}}{4}\right)^2} - \frac{\sqrt{17}-1}{4} \right) = \\
&= \frac{R}{2} \left( \sqrt{\frac{81-9\sqrt{17}}{8}} - \frac{\sqrt{17}-1}{4} \right) = \\
&= \frac{\sqrt{17}-1}{4} R
\end{aligned} \tag{22}$$

From equations (21) and (22):

$$\frac{\max C_x}{E_C} \leq 2 \frac{w}{\pi^2 w} = 2\pi^{-2} \tag{23}$$

where

$$w = \frac{\sqrt{17}-1}{4} R \tag{24}$$

■

#### 4. Application

The proposed theory includes the following hypotheses that require experimental evaluation. The worst-case considered is based on a continuous feature, consequently, equiangular data and large datasets are necessary for real applications.

The condition of uniformly distributed sampled points is fundamental because the centroid position could be influenced more by the sampled points distribution than from the sphericity error to be assessed. The acquisition of equiangular datapoints is a common strategy in metrology and reverse

engineering [22] [23] and does not seem a limitation for the industrial application of the proposed theory, except in the case of partial (or incomplete) features, discussed below.

As for the dataset size, the proposed upper bound has been applied on artificially generated datasets as discussed in the next section. Furthermore, to experimentally assess the proposed search neighborhood for the minimum zone center  $C_{MZ}$  with center-based algorithms, such as genetic algorithms, ant colony systems, particle swarm optimization, taboo search etc. a genetic algorithm with parameters previously optimized for the roundness problem [11] has been extended to three dimensions. Genetic algorithms constitute a class of implicit parallel search methods especially suited for solving complex optimization or non-linear problems. They are easily implemented and powerful being a general-purpose optimization tool. Many possible solutions are processed concurrently and evolve with inheritable rules, e.g. the elitist or the roulette wheel selection, so to quickly converge to a solution, which is very close or coincident to the optimal solution.

In [24], it has been proven that, for genetic algorithms, parents of the first generation included in the cube circumscribed to the spherical search neighborhood, generate offspring included in the same (or smaller) space. This *convergence condition* should be verified by the search mechanism of other algorithms considered.

To show a possible application of the method and to provide some orders of magnitude of the estimation of the minimum zone center  $C_{MZ}$  in different case studies found by different authors, its distance  $|C-C_{MZ}|$  from the centroid  $C$  on datasets from the literature has been compared with the upper bound  $2 \pi^2 E_C$  predicted by the theory proven in the previous sections.

## 5. Computation experiments with artificially generated datasets

For the application of the proposed upper bound on artificially generated datasets, the NPL Chebyshev best fit circle *certified* software [25] cannot be used without post-processing, because not only the distribution of the radiuses of points is random, but also their angle, consequently the hypothesis of equiangular distribution is not verified. Possible post-processing includes the relocation of the angular position of the datapoints, including those satisfying the 1-3, 3-1 or 2-2 conditions according to [26], after conversion to polar coordinates using the given  $C_{MZ}$  as the reference origin.

As an alternative, a simple program [27] has been implemented to generate equiangular datasets of given size  $n$ , on three roundness profiles on the XY-, XZ- and YZ-planes. The listing is available for direct execution in Appendix and it can be used with given random seeds.

The centroid  $C_n$  for a set of  $n$  points sampled on a spherical surface is

$$C_n = \frac{1}{n} \begin{bmatrix} \sum_{i=1}^n \sum_{j=1}^{n/2} s(x, y, z, \theta_i, \varphi_j) \cos \theta_i \cos \varphi_j \\ \sum_{i=1}^n \sum_{j=1}^{n/2} s(x, y, z, \theta_i, \varphi_j) \sin \theta_i \cos \varphi_j \\ \sum_{i=1}^n \sum_{j=1}^{n/2} s(x, y, z, \theta_i, \varphi_j) \sin \varphi_j \end{bmatrix} \quad (25)$$

$E_{C_n}$  can be determined from (1) and (25) by

$$\begin{aligned} E_{C_n} &= R_{\max}(C_n) - R_{\min}(C_n) = \\ &= \max_{\theta_i = i \frac{2\pi}{n}, i=1, \dots, n, \varphi_j = j \frac{2\pi}{n}, j=1, \dots, \frac{n}{2}} s(C_n, \theta_i, \varphi_j) - \min_{\theta_i = i \frac{2\pi}{n}, i=1, \dots, n, \varphi_j = j \frac{2\pi}{n}, j=1, \dots, \frac{n}{2}} s(C_n, \theta_i, \varphi_j) \end{aligned} \quad (26)$$

The *exact* minimum zone center  $C_{MZ}$  of artificial datasets is known by construction, by applying the 2-2 condition in [26]. The result of this numerical analysis on random data is represented in Figure 4, where the position of the minimum zone center within the (theoretical) search area  $S$  is compared with the theoretical spherical radius of  $2 \pi^2 E_{C_n}$  obtained with artificial datasets, which can be reproduced with the parameters in caption.



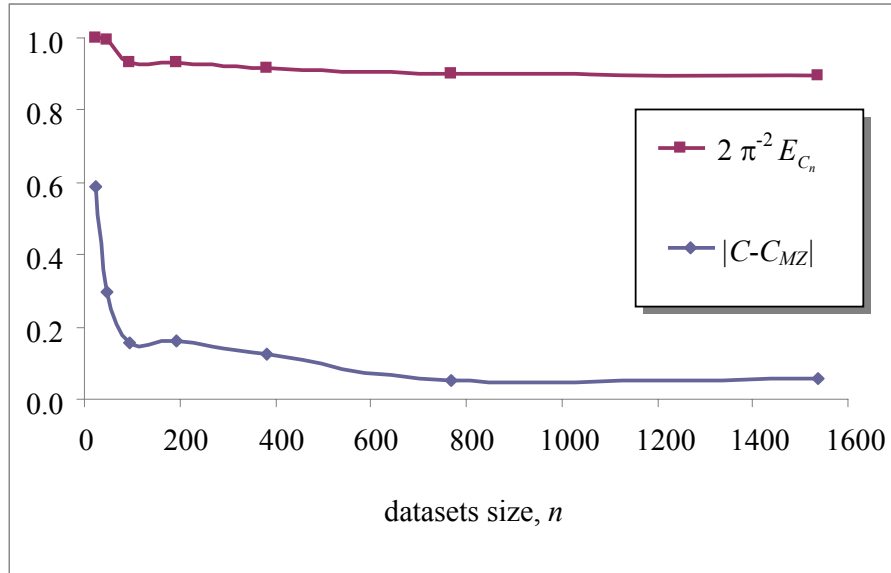


Figure 4: Effect of the proposed upper bound for the  $|C-C_{MZ}|$  distance with datasets artificially generated as in Appendix [27], for different values of  $n$  ( $\times 3$ ) = 8, 16, 32, 64, 128, 256, 512,  $C_{MZ}=(0,0,0)$ , random seed=0 (XY-plane), 1 (XZ-plane), 2 (YZ-plane), nominal radius  $R_n = 20$ ,  $E_{MZ} = 0.02$ . Data are normalized to the maximum:  $2 \pi^2 E_{C_n}$  ( $n = 24$ ) = 0.0046.

About here

From Figure 4, it can be clearly observed that the search space size and the minimum zone to centroid distance have a similar trend with the increase of the dataset size; the amount of the overestimate (in the range 6 to 59%) is also visible.

The decreasing trend of  $|C-C_{MZ}|$  is not strictly monotonous (e.g. from 96 and 192 and from 768 and 1536), as opposed to real features at increasing sample rate, e.g. characterized by a manufacturing based signature [28] [29]). The random generation of artificially generated datapoints does not necessarily increase the accuracy of the description of the same profile of a feature; instead, artificial profiles with increasing random generated datapoints can be seen more as profiles of different features. This phenomenon is also described by the displacement of the control point described in the Proposition and shown in Figure A1 in Appendix A of [21], which can be seen as the effect of the profile signature on the form tolerance.

The sharp decrease before 96 datapoints is probably due to the beneficial increase of the sampling error as a function of the required tolerance to be assessed and seems an optimum compromise between dataset size and accuracy.

## 6. Computation experiments with datasets from the literature

All the (five) datasets available from the literature, which have been tested with center-based methods and where the minimum zone center  $C_{MZ}$  is declared, are listed in Table 1 with the reference to the original works and with the results achieved by other authors by their respective methods. Minimum zone centers are not available from [7], [30] and [31], and from the authors of dataset 1 [14].

A genetic algorithm, with parameters previously optimized in [24] for roundness, has been used for minimum zone sphericity assessment with the addition of the third chromosome (coordinate  $Z$ ) and is listed.

Unfortunately, no datasets are equiangular. For the above-mentioned reason, the sampled points distribution influences the centroid position up to one order of magnitude higher than the minimum zone error  $E_{MZ}$  to be assessed. Because of the lower influence of the sampled points distribution on the least squares center  $C_{LS}$  and error  $E_{LS}$ , in Table 1 they have been used as estimators for the centroid  $C$  and of the sphericity error with respect to the centroid  $E_C$ .

From Table 1 it can be noticed that, not only all values for the *difference* parameter are positive, but also that they almost exploit all the available range (between 22.12% of cases # 1.2 and 1.3 and 99.62% of case # 1.7) and make it a very tight upper bound. In this regard, the least squares center  $C_{LS}$  and error  $E_{LS}$  can be considered good estimators for the centroid  $C$  and error  $E_C$ .

The genetic algorithm in [24] extended from roundness to the three dimensional problem has achieved the following minimum zone errors  $E_{MZ}$  on the five datasets from the literature detailed in Table 1: **0.00766**, 0.008329 (**0.008329** [14]), 0.0096779 (**0.00966** [8]), **1.0000**, 3.407569 (**3.332518** [20]). The current best known results in bold have also been indicated. This shows that the proposed genetic parameters optimized for roundness are effective for the sphericity problem as well.

## 7. Computation experiments with real datasets

The same genetic algorithm has been tested on four new real datasets summarized in Table 2. The processing time of the proposed genetic algorithm along with the minimum zone error  $E_{MZ}$  and radius  $r_{MZ}$  have been provided. The raw sampled data are available as supplementary material. The recommendation on the dataset size coming from experiments on artificial datasets of about one hundred sampled points has been followed; however the less favorable conditions of not equiangular distribution and partial feature sampling have been applied.

From Table 2 it can be noticed that again all values for the *difference* parameter are positive. It can also be observed that they exploit a wide range of available values (between 1.67% of case 7 to 61.82% of case 8).

The parameter  $E_{MZ}/E_{LS}$  is a quantitative estimate of the benefit of using the MZ versus the least squares criterion for part inspection, yielding between 10% (case 8) to 18.50% (case 7) more of acceptable parts.

The *difference* and the  $E_{MZ}/E_{LS}$  parameters (last two columns of Table 2) show a mild direct correlation also found on the dataset in Table 1, which seems reasonable, but requires further investigation.

Accepted Manuscript

Table 1: The proposed upper bound ( $2 \pi^2 E_C$ ) compared with the distance between centroid  $C$  and minimum zone center  $C_{MZ} \equiv (x_{MZ}, y_{MZ}, z_{MZ})$  estimated by different authors on five spherical surfaces from the literature. The least squares center  $(x_{LS}, y_{LS}, z_{LS})$  and the least squares error  $E_{LS}$  are considered to estimate the *difference* =  $2 \pi^2 E_C - |C - C_{MZ}|$ . Rounding is as given in references.

| dataset #/ref. | $n$ | $x_{LS}$  | $y_{LS}$  | $z_{LS}$   | $E_{LS}$ | case # | ref. | algorithm | $x_{MZ}$  | $y_{MZ}$      | $z_{MZ}$   | $ C - C_{MZ} $ | $2 \pi^2 E_C$ | <i>difference</i> | <i>difference</i><br>$2 \pi^2 E_C$ |
|----------------|-----|-----------|-----------|------------|----------|--------|------|-----------|-----------|---------------|------------|----------------|---------------|-------------------|------------------------------------|
| 1 [14]         | 50  | 0.00085   | -0.00037  | 0.00078    | 0.00849  | 1.1.   | [8]  | IEA       | 0.002495  | -0.000097     | 0.000479   | 0.001330887    | 0.001720434   | +0.000389546      | 22.64%                             |
|                |     |           |           |            |          | 1.2.   | [10] | GA        | 0.0025    | -0.0001       | 0.0005     | 0.001339942    | 0.001720434   | +0.000380491      | 22.12%                             |
|                |     |           |           |            |          | 1.3.   | [16] | Limacoid  | 0.0025    | -0.0001       | 0.0005     | 0.001339942    | 0.001720434   | +0.000380491      | 22.12%                             |
|                |     |           |           |            |          | 1.4.   | [18] | GA        | 0.000993  | 0.000024      | 0.000058   | 0.000216546    | 0.001720434   | +0.001503888      | 87.41%                             |
|                |     |           |           |            |          | 1.5.   | [20] | PSO       | 0.002506  | -0.000097     | 0.000481   | 0.001342059    | 0.001720434   | +0.000378375      | 21.99%                             |
|                |     |           |           |            |          | 1.6.   | [24] | GA        | 0.0025    | -0.0001       | 0.0005     | 0.001339942    | 0.001720434   | +0.000380491      | 22.12%                             |
|                |     |           |           |            |          | 1.7.   | [32] | IEA       | 0.001118  | 0.000414<br>9 | -0.0001727 | 6.58344E-06    | 0.001720434   | +0.00171385       | 99.62%                             |
| 2 [15]         | 40  | 0.0041    | 0.0033    | 0.0035     | 0.0090   | 2.1.   | [8]  | IEA       | 0.003910  | 0.002536      | 0.004556   | 0.000196801    | 0.001823781   | +0.00162698       | 89.21%                             |
|                |     |           |           |            |          | 2.2.   | [10] | GA        | 0.0039    | 0.0025        | 0.0046     | 0.000207798    | 0.001823781   | +0.001615983      | 88.61%                             |
|                |     |           |           |            |          | 2.3.   | [15] | Analytic  | 0.003911  | 0.002535      | 0.004562   | 0.000207798    | 0.001823781   | +0.001615983      | 88.61%                             |
|                |     |           |           |            |          | 2.4.   | [24] | GA        | 0.0039    | 0.0025        | 0.0046     | 0.000201208    | 0.001823781   | +0.001622574      | 88.97%                             |
| 3 [15]         | 36  | 0.0006    | -0.0029   | -0.00001   | 0.0132   | 3.1.   | [8]  | IEA       | 0.003506  | -0.003308     | -0.000292  | 0.00186766     | 0.002674879   | +0.000807219      | 30.18%                             |
|                |     |           |           |            |          | 3.2.   | [10] | GA        | 0.0038    | -0.0031       | -0.0001    | 0.001943664    | 0.002674879   | +0.000731215      | 27.34%                             |
|                |     |           |           |            |          | 3.3.   | [15] | Analytic  | 0.003509  | -0.003305     | -0.000292  | 0.001943664    | 0.002674879   | +0.000731215      | 27.34%                             |
|                |     |           |           |            |          | 3.4.   | [24] | GA        | 0.0038    | -0.0031       | -0.0001    | 0.001867785    | 0.002674879   | +0.000807094      | 30.17%                             |
| 4 [13]         | 100 | -0.0191   | 0.0893    | 0.0176     | 1.1522   | 4.1.   | [10] | GA        | 0         | 0             | 0          | 0.093000323    | 0.233484536   | +0.140484213      | 60.17%                             |
|                |     |           |           |            |          | 4.2.   | [13] | Voronoi   | 0         | 0             | 0          | 0.093000323    | 0.233484536   | +0.140484213      | 60.17%                             |
|                |     |           |           |            |          | 4.3.   | [24] | GA        | 0         | 0             | 0          | 0.093000323    | 0.233484536   | +0.140484213      | 60.17%                             |
| 5 [18]         | 25  | -0.284417 | -0.662540 | -0.0568719 | 3.618231 | 5.1.   | [18] | GA        | -0.412356 | -0.335014     | -0.326140  | 0.09983803     | 0.733206895   | +0.633368865      | 86.38%                             |
|                |     |           |           |            |          | 5.2.   | [20] | PSO       | -0.388729 | -0.355488     | -0.299887  | 0.284379168    | 0.733206895   | +0.448827727      | 61.21%                             |
|                |     |           |           |            |          | 5.3.   | [24] | GA        | -0.2751   | -0.2675       | -0.2130    | 0.117100342    | 0.733206895   | +0.616106553      | 84.03%                             |

Table 2: The proposed upper bound ( $2 \pi^2 E_C$ ) compared with the distance between centroid  $C$  and minimum zone center  $C_{MZ} \equiv (x_{MZ}, y_{MZ}, z_{MZ})$  estimated on four new spherical surfaces from real parts. The least squares center  $(x_{LS}, y_{LS}, z_{LS})$  and the least squares error  $E_{LS}$  are considered to estimate the *difference* =  $2 \pi^2 E_C - |C - C_{MZ}|$ .

| dataset # | item                 | Partial feature   | $n$ | $x_{LS}$ | $y_{LS}$ | $z_{LS}$ | $E_{LS}$ | $r_{LS}$ | time  | $x_{MZ}$    | $y_{MZ}$ | $z_{MZ}$ | $E_{MZ}$ | $r_{MZ}$ | $ C - C_{MZ} $ | $2 \pi^2 E_C$ | difference | $\frac{\text{difference}}{2 \pi^2 E_C}$ | $\frac{E_{MZ}}{E_{LS}}$ |
|-----------|----------------------|-------------------|-----|----------|----------|----------|----------|----------|-------|-------------|----------|----------|----------|----------|----------------|---------------|------------|---|-------------------------|
| 6         | spherical joint      | hemisphere        | 100 | 0        | 0        | 0        | 0.046    | 27.4685  | 0.109 | -<br>0.0003 | 0.0084   | 0.0018   | 0.0401   | 27.4637  | 0.00859593     | 0.009322      | 0.000726   | 7.78%                                   | 87.17%                  |
| 7         | eccentric cam        | spherical segment | 79  | 0        | 0        | 0        | 0.040    | 22.047   | 0.078 | 0.0034      | 0.0066   | 0.0029   | 0.0326   | 22.046   | 0.00797057     | 0.008106      | 0.000135   | 1.67%                                   | 81.50%                  |
| 8         | qualification sphere | hemisphere        | 99  | 0        | 0        | 0        | 0.017    | 32.1325  | 0.094 | 0.0012      | 0.0002   | 0.0005   | 0.0153   | 32.1472  | 0.00131529     | 0.003445      | 0.00213    | 61.82%                                  | 90.00%                  |
| 9         | billiard ball        | hemisphere        | 99  | 0        | 0        | 0        | 0.053    | 30.3345  | 0.110 | 0.0015      | 0.0045   | 0.0077   | 0.0466   | 30.3317  | 0.00904378     | 0.01074       | 0.001696   | 15.79%                                  | 87.92%                  |

## 8. Conclusions

The minimum zone tolerance  $E_{MZ}$  is determined by the two concentric spherical surfaces, with minimum radial separation or minimum zone error, centered in the minimum zone center  $C_{MZ}$ . The worst-case, described in Figure 2, has been built to estimate the maximum distance (upper bound) of the (unknown) minimum zone center from the centroid (known, by expression (25) for equiangular datapoints, otherwise estimated by the least squares method).

This distance can be used as the radius of a spherical search neighborhood, e.g. for center-based algorithms, and equals  $2\pi^2 E_C$ , where  $E_C$  is the sphericity error related to the centroid, which can be evaluated in closed form, from expression (26).

As opposed to past research, not only the search space size is adaptable, but there is also no risk that the minimum zone center to be searched is outside.

The funding hypothesis of continuous profiles, can be easily coped with current equiangular sampling strategies applied in metrology and reverse engineering.

Experimental tests with all (five) available datasets from the literature and four new sampled datasets have shown that the upper bound estimated by the least square error is able to overestimate the  $C_{LS}$  to  $C_{MZ}$  distance in the whole range up to almost 100%, making it a *tight* upper bound.

A direct correlation between “how much” of the search space is used (the *difference* parameter) and the benefit of using the MZ versus the least squares criterion (the  $E_{MZ}/E_{LS}$  parameter) has been observed and requires further investigation both under the experimental and theoretical viewpoints. Computation experiments have also shown that the least square center  $C_{LS}$  and error  $E_{LS}$  are good estimators of the centroid  $C$  and error  $E_C$ . This makes the proposed upper bound potentially suitable for partial features, where the uniform datapoint distribution hypothesis is not satisfied. Future research may address the quantitative evaluation of the distribution and uniformity by the proposed upper bound, e.g. as a norm involving a combination of  $C$  and  $C_{LS}$  to compare the sphericity error versus the sampling error.

The genetic algorithm previously optimized by the authors for the roundness problem and adapted to the three dimensional problem has been confirmed to be fast (below one second processing time) and shown to meet or exceed the competing center-based algorithms for sphericity evaluation on the mentioned datasets.

Existing and future minimum zone center-based algorithms and algorithms that approach the minimum zone method by iterative center evaluations (e.g. the mentioned genetic algorithms and other metaheuristics) can benefit of the lower search space size to a neighbor of the centroid  $C$ .

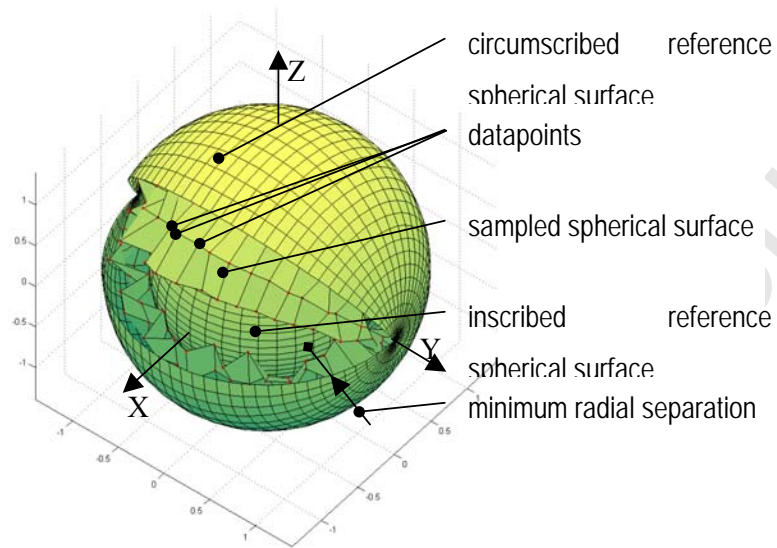
### **9. Acknowledgement**

This work has been carried out as Stefano Chiodi's project work in Automation of Manufacturing Processes 2010-11 for the master degree in Automation Engineering at Pisa University.

### **10. References**

Accepted Manuscript

## Graphical abstract





### Highlights

worst-case (upper bound) for the centroid to minimum zone center distance

search neighborhood containing the minimum zone center (MZC)

closed form estimation of the MZC for center-based algorithms (GA, PSO, ACO etc.)

Accepted Manuscript

## 11.

- [1] ASME B89.3.1 Measurement of Out-Of-Roundness. 2003.
- [2] ISO 1101, Geometrical Product Specifications (GPS)–tolerances of form, orientation, location and run out, 2nd ed. International Organization for Standardization, Geneva, Switzerland, 2004, December.
- [3] Weber T., Motavalli S., Fallahi B., Cheraghi S.H. A unified approach to form error evaluation. *Journal of the International Societies for Precision Engineering and Nanotechnology* 2002;26:269–278.
- [4] Murthy T.S.R., Abdin S.Z. Minimum zone evaluation of surfaces, *International Journal of Machine Tool Design Research* 1980;20:123–136.
- [5] Kovvur Y., Ramaswami H., Anand B.R., Anand S., Minimum-zone form tolerance evaluation using particle swarm optimisation, *International Journal of Intelligent Systems Technologies and Applications*, 2008;4(1/2).
- [6] Mao J., Cao Y., Yang J. Implementation uncertainty evaluation of cylindricity errors based on geometrical product specification (GPS), *Measurement*, 2009;42(June(5)):742-747.
- [7] Ke Z. Minimum Zone Evaluation of Sphericity Error Based on Ant Colony Algorithm. In *Electronic Measurement and Instruments*, 2007. ICEMI'07. 8th International Conference on 2007; August:2-535.
- [8] Wen X.L., Song A. An immune evolutionary algorithm for sphericity error evaluation. *International Journal of Machine Tools and Manufacture* 2004;44:1077–1084.
- [9] Jianxi P., Xiao Y., Jianping L., ZhiYuan L. Research of sphericity error evaluation method of calculating the uncertainty in the specification, *Computational Intelligence and Design (ISCID)*, 2011 Fourth International Symposium on. 2011.
- [10] Chen M.-C. Analysis of Spherical Form Errors to Coordinate Measuring Machine Data. *JSME International Journal* 2002; Series C 45(2):647-656.
- [11] Rossi A., Antonetti M., Barloscio M., Lanzetta M. Fast genetic algorithm for roundness evaluation by the minimum zone tolerance (MZT) method. *Measurement* 2011;44(August(7)):1243-1252, <http://dx.doi.org/10.1016/j.measurement.2011.03.031>.
- [12] Meo A., Profumo L., Rossi A., Lanzetta M. Optimum Dataset Size and Search Space for Minimum Zone Roundness Evaluation by Genetic Algorithm. *Measurement Science Review* 2013;13(3):100-107, <http://dx.doi.org/10.2478/msr-2013-0018>.

- [13] Huang J. An exact minimum zone solution for sphericity evaluation. *Computer-Aided Design* 1999;31:845–853.
- [14] Fan K.-C., Lee J.-C. Analysis of minimum zone sphericity error using minimum potential energy theory, *Precision Engineering* 1999;23:65–72.
- [15] Chen C.K., Liu C.H. A study on analyzing the problem of the spherical form error. *Precision Engineering* 2000;24:119–126.
- [16] Samuel G.L., Shunmugam M.S. Evaluation of circularity and sphericity from coordinate measurement data, *Journal of Materials Processing Technology* 2003;139:90–95.
- [17] Lai H.-Y., Jywe W.-Y., Chen C.-K., Liu C.-H. Precision modeling of form errors for cylindricity evaluation using genetic algorithms. *Precision Engineering* 2000;24(4):310-319.
- [18] Cui C.-C., Che R.-S., Ye D., Huang Q.-C. Sphericity error evaluation using the genetic algorithm. *Optics and Precision Engineering* 2002;10(4):333-339.
- [19] Wen X.L., Song A. An improved genetic algorithm for sphericity error evaluation. In *Neural Networks and Signal Processing, 2003. Proceedings of the IEEE International Conference 2003(December)*;1:549-553).
- [20] Wen X., Li H., Wang F., Wang D. Sphericity Error United Evaluation Using Particle Swarm Optimization Technique. *Electronic Measurement & Instruments ICEMI'2009, The Ninth International Conference on, 2009*;1-156.
- [21] Rossi A., Lanzetta M. Roundness: a closed form upper bound for the centroid to minimum zone center distance by worst-case analysis, *Measurement*, 2013;46(7):2251-2258, <http://dx.doi.org/10.1016/j.measurement.2013.03.025>.
- [22] Weckenmann A., Knauer M., Kunzmann H. The influence of measurement strategy on the uncertainty of CMM-measurements, *CIRP Annals-Manufacturing Technology*, 1998;47(1):451-454.
- [23] Weckenmann A., Weber H., Eitzert H., Garmer M. Functionality-oriented evaluation and sampling strategy in coordinate metrology, *Precision Engineering* 1995;17(4):244–52.
- [24] Rossi A., Lanzetta M. Optimal blind sampling strategy for minimum zone roundness evaluation by metaheuristics, *Precision Engineering* 2013;37(2):241-247 <http://dx.doi.org/10.1016/j.precisioneng.2012.09.001>.
- [25] National Physical Laboratory (UK), Data Generator for Chebyshev Best-Fit Circle, <http://www.npl.co.uk/mathematics-scientific-computing/software-support-for-metrology>.

- [26] Jywe W.-Y., Liu G.-H, Chen C.-K. The min-max problem for evaluating the form error of a circle. *Measurement* 1999;26:273-282.
- [27] Mathworks™, Matlab®.
- [28] Rossi A. A form of deviation-based method for coordinate measuring machine sampling optimization in an assessment of roundness. *Proceedings of the Institution of Mechanical Engineers, Part B: Journal of Engineering Manufacture* 2001;215(11):1505–1518.
- [29] Rossi A. A minimal inspection sampling technique for roundness evaluation. In 1st CIRP International Seminar on Progress in Innovative Manufacturing Engineering (Prime), 20-22 June 2001:189-196.
- [30] Saravanan S. Evaluation of Sphericity Using Modified Sequential Linear Programming, Master thesis, Univ. of Cincinnati 2004.
- [31] Prisco U., Polini W., Flatness, Cylindricity and Sphericity Assessment Based on the Seven Classes of Symmetry of the Surfaces. *Advances in Mechanical Engineering* 2010;2010, <http://dx.doi.org/10.1155/2010/154287>.
- [32] Samuel G.L., Shunmugam M.S. Evaluation of sphericity error from form data using computational geometric techniques. *International Journal of Machine Tools and Manufacture* 2002;42:405–416.